Available online at www.sciencedirect.com

ScienceDirect

IFAC Papers Online CONFERENCE PAPER ARCHIVE

IFAC-PapersOnLine 48-11 (2015) 078–085

Dynamical modeling for electric hot water tanks

Nathanael Beeker * **Paul Malisani** ** **Nicolas Petit** ***

* *EDF Lab, EnerBat, Avenue des Renardières - Ecuelles, 77818 Moret-sur-Loing Cedex FRANCE (e-mail: nathanael.beeker-adda@edf.fr)*
** *EDF Lab, EnerBat, Avenue des Renardières - Ecuelles, 77818 Moret-sur-Loing Cedex FRANCE (e-mail: paul.malisani@edf.fr).*
*** *MINES ParisTech, CAS, 60 bd Saint-Michel, 75272 Paris Cedex FRANCE (e-mail: nicolas.petit@mines-paristech.fr)*

Abstract: To quantify the potential of electric hot water tanks (EHWT) in general demand response programs, there is a need for models with prediction capabilities at a reasonable computational cost. As can be experimentally observed, the input-output response of EHWT is relatively complex. This paper presents two models of EHWT, one in the form of two simple one-dimensional partial differential equations and the other as a hybrid system decoupling the phenomena acting on the EHWT, in sequences. An experimental validation compares the performance of these models. The conclusion is that the hybrid model is more accurate and less computationally intensive.

Keywords: Electric hot water tank, distributed parameter systems, hybrid modeling, nonlinear systems, load shifting.

1. INTRODUCTION

The increasing share of intermittent renewable electricity sources in the energy mix (Commission [2011], Edenhofer et al. [2011]) reveals troublesomefor managing the electricity production-consumption equilibrium. This status can be observed at national and local levels. Demand Side Management (DSM), which is a portfolio of techniques aiming at tailoring consumers' demand, is a promising solution for such concerns (Palensky and Dietrich [2011]). A key factor in developing DSM is the availability of energy storage capacities. For this reason, network operators and electricity producers are developing new ways of storing energy. In this context, the large pools of electric hot water tanks (EHWT) found in numerous countries (the market share of electric heater being 35% in Canada, see Aguilar et al. [2005], 38% in the U.S, see Ryan et al. [2010], and 45% in France, see MSI [2013]) is particularly appealing. For load shifting applications, its large storage capacities, the flexibility yielded by its geographically scattered characteristic and its functioning are key enabling factors.

EHWTs heat water over relatively long periods of time. To minimize cost, electricity is used in the night time (one period when electricity price is low), while hot water is used in the next day-time. More advanced timing strategies are believed to generate further cost-reductions. Design of these strategies requires dynamical models, e.g. to determine optimal heating periods in response to fluctuating prices of electricity. In this paper, we develop one such model.

An EHWT can be seen as a two inputs, single output dynamical system. The two inputs are the heating power and water outflow (or drain). The output is the distribution of temperature of water in the tank, which can be used to define, for optimization purposes, quality of service indexes. This simple description should not suggest that the internal system dynamics are straightforward. In this paper, we will consider a natural performance index, the "available energy", representing the total energy contained in the water whose temperature is above some prescribed threshold (e.g. 40°C). The rationale behind this choice is that hot water can be used by blending it with cold water for all domestic purposes, provided its temperature is above the desired threshold. As will appear, accurate forecasting of this variable requires advanced modeling.

In the literature (Blandin [2010], Kleinbach et al. [1993], Zurigat et al. [1991]), hot water storages are modeled as vertical cylindrical columns driven by thermo-hydraulic phenomena: heat diffusion, buoyancy effects and induced convection and mixing, forced convection induced by draining and associated mixing, and heat loss at the walls. Most existing models are either *i)* one-dimensional superposition of layers (see e.g. Blandin [2010]), or *ii)* three or two-dimensional (using rotational symmetry) models, often using a discretization for numerical simulation purposes such as computational fluid dynamics (Blandin [2010], Han et al. [2009], Johannes et al. [2005]) or *iii)* so-called zonal models often based on the software TRNSYS (Johannes et al. [2005], Klein et al. [2010]). These models, although accurate, are numerically intensive and do not fit with our requirements of numerical efficiency. On the other hand, when overly simplified, these layers models fail to reproduce some physical phenomena whose effects are observed in practice. This is particularly true in

2405-8963
Peer review under responsibility of International Federation of Automatic Control.
10.1016/j.ifacol.2015.09.163

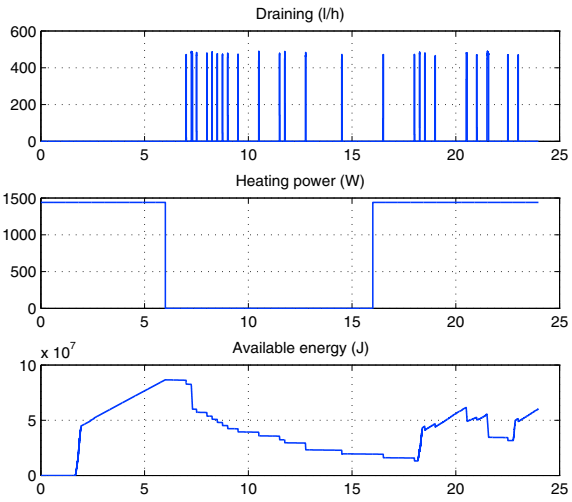

Fig. 1. Available hot water as a function of heating and draining on a 24h run (experimental data). The system is initially uniformly cold.

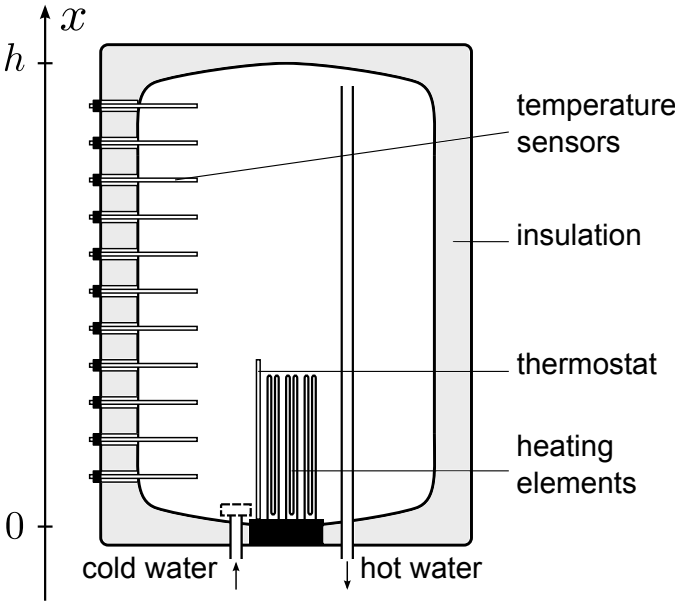

Fig. 2. Schematic view of an EHWT.

our context when one wishes to introduce heating in the dynamics.

A complexity trade-off must be found. Interestingly, a careful study of the physical principles at stake in the system suggests some simplifications. The buoyancy effects lead to the so-called stratification phenomenon (Han et al. [2009]), causing horizontal homogeneity of the temperature profile, increasing with height. This effect is dominant and allows one to consider only one-dimensional models. Following this approach, the first model we briefly develop here extends an existing one-dimensional convection-diffusion linear equation modeling the draining convection and its mixing developed in the 1980s (Zurigat et al. [1988, 1991]). In details, to the classic governing equation, we add a nonlinear velocity term given by empirical laws lumping various phenomena (turbulent natural convection due to heating in particular). Further, we introduce heating power as a source term. Experimental data illustrate the relevance of this modeling. The model is concise, and relatively accurate. However, several improvements are possible.

Then, in a second step, we decouple heating and draining effects and develop a model based on the decomposition of the dynamics according to the dominant effect at stake. We distinguish three phases: heating, draining and rest. For heating, we reproduce a behavior observed in experimental data in which the temperature increases first at the bottom of the tank forming a spatially uniform temperature distribution which gradually extends itself upwards to the top of the tank. We explain this observation by a model of buoyancy-induced forces, generating a local natural convection phenomenon. This homogeneous zone is followed by an increasing profile of temperature in the upper part of the tank, remaining untouched due to stratification (heat diffusion being neglected in this case). Draining is treated as a convection parameter and its associated mixing effects are reproduced by a diffusion term following the approach of Zurigat et al. [1991]. We model the effects of the water nozzle which creates a mixing zone of varying temperature and volume. The cascade represents a Stefan problem (Fasano and Primicerio [1977a,b]). Finally, rest phases are simply driven by diffusion and loss. Sequencing the three phases constitutes a hybrid model.

This hybrid model is the main contribution of this article. It kindly reproduces experimental data presented in this article, and permits to compute the dynamics of the "available energy", defined earlier, in response to the water drain and the power injected in the tank. A typical scenario is reported in Fig.1. As it is visible, the input-output behavior of the system in somewhat complex although not counter-intuitive [1] .

The paper is organized as follows. After having described the first model, we illustrate it by means of simulations and compare it against experimental data in Section 2. In this study, a typical 200L tank (equipped with spatially distributed internal sensors) with realistic scenarios of draining and heating is employed. Section 3 is dedicated to the presentation of the hybrid model which is the main contribution of the paper. Comparative studies reported in Section 4 conclude that this hybrid model is more accurate and more computationally efficient.

2. PRELIMINARY CONSIDERATIONS AND FIRST MODELING

2.1 General considerations on water tanks and stratification

A typical EHWT is a vertical cylindrical tank filled with water in which a heating element is plunged at the bottom end (see Fig. 2). The heating element is pole-shaped, and its length is relatively large, up to one third of the tank. Cold water is injected at the bottom while hot water

[1] Heating water takes time. Starting from a uniformly cold tank, the output of the system (the "available energy") remains identically equal to zero for hours. Then it jumps, and steadily increases. Draining causes steps down on the output, and also causes some internal mixing which is non negligible.

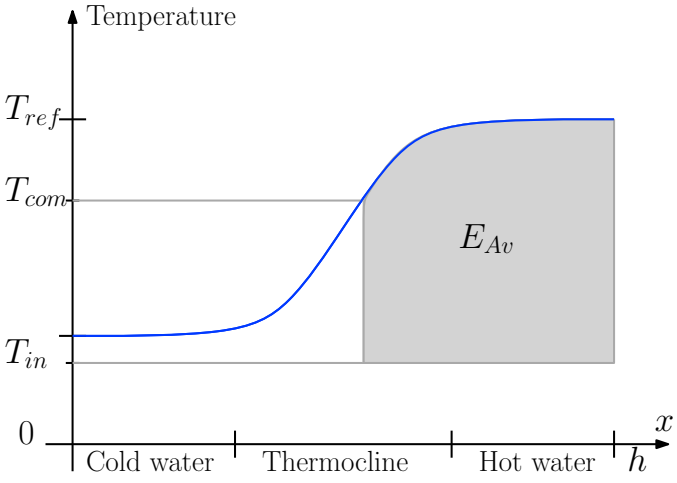

Fig. 3. Example of the temperature profile inside a stratified water tank.

is drained from the top at exactly the same flow rate (under the assumption of pressure equilibrium in the water distribution system). Therefore, the tank is always full. In the tank, layers of water with various temperature can coexist (see Fig.3). At rest, these layers are mixed only by heat diffusion which effects are relatively slow (Han et al. [2009]). Existence of a non uniform (increasing with height) quasi-equilibrium temperature profile in the tank is called *stratification* (Dincer and Rosen [2010], Han et al. [2009], Lavan and Thompson [1977]). In practice, this effect is beneficial for the user as hot water available for consumption is naturally stored near the outlet of the EHWT, while the rest of the tank is heated (see Fig.3). Due to this effect and the cylindrical symmetry of the system, one can assume that the water temperature in the tank is homogeneous at each height of the tank and one can limit studies to one-dimensional models.

2.2 Coupled one-dimensionnal distributed parameters model

The system can be described by coupled diffusion-convection Partial Differential Equations (PDEs). To account for heating buoyancy effects, one of the convection parameter is impacted by the local temperature increase. Defining two states $T, \Delta T$ standing for average and spread of temperature, respectively, we have

$$\begin{aligned}
\partial_t T + \partial_x(v_d T) &= \alpha \partial_{xx} T + \Phi \Delta T - k(T - T_a) \\
\partial_t \Delta T + \partial_x((v_d + v_{nc})\Delta T) &= \alpha \partial_{xx} \Delta T - \Phi \Delta T + P_W \\
v_d(T(0,t) - T_{in}) + \alpha \partial_x T(0,t) &= 0 \\
v_d \Delta T(0,t) + \alpha \partial_x \Delta T(0,t) &= 0 \\
\partial_x T(h,t) &= 0 \\
\partial_x \Delta T(h,t) &= 0 \\
T(x,t_0) &= T_0(x)
\end{aligned} \tag{2.1}$$

where $v_d \geq 0$ is the velocity induced by the draining (assumed spatially uniform but time-varying), $\alpha = \alpha_t + \alpha_d$ is the sum of the thermal diffusivity of water and an additional turbulent diffusivity representing the drain mixing effects, k is a coefficient scaling the loss to the exterior assumed to be at constant temperature T_a, and T_{in} is the temperature of injected water. To these term representing draining, heat loss and thermal diffusion, we add a velocity term v_{nc} of natural convection, which is responsible for transport of energy in the system, a distributed heat exchange term $\Phi \Delta T$ representing at each height the mixing induced by natural convection which is proportional to the temperature spread, and the spatially distributed source term P_W (representing the power injected in the tank via the heating elements), which drives the dynamic of ΔT. The nonlinear transport velocity v_{nc} and exchange coefficient Φ between the two equations are modeled as

$$v_{nc}(x,t) = v\Big(\int_x^h [T(x,t) + \Delta T(y,t) - T(y,t)]_+^\beta dy\Big)^\gamma \tag{2.2}$$

$$\Phi(x,t) = \phi[v_{max} - v_{nc}(x,t)]_+ \tag{2.3}$$

where $[z]_+$ is the positive part of z and v, ϕ, v_{max}, β and γ are positive factors.

For more details about the model and the derivation of equations (2.1-2.3), the interested reader is referred to Beeker et al. [2015].

2.3 First comparison against data: some limitations appear

To validate the model, experiments have been conducted in the facilities of EDF Lab Research Center, on an Atlantis ATLANTIC VMRSEL 200L water tank. The power is injected via three nearby elements permitting a power injection up to 2200W. The dimensions of the water tank are specified in Table 1.

Table 1. Specifications of the EHWT used in experiments

Volume (L)	200
Length (m)	1.37
Maximal power (W)	2200
Heat loss coefficient ($WK^{-1}m^{-2}$)	0.66

The water tank has been equipped with internal temperature sensors to record temperature at 15 locations of different heights, 15cm deep inside the water tank (see Fig. 2). This depth is sufficient to bypass the insulation of the tank. Reasonably, it can be assumed that the sensors have no effect on the flows (e.g. that they do not induce significant drag). During the experiment, the following quantities have been measured with external sensors: injected power, water flow at the inlet, water temperature at the inlet. These three quantities feed the model, the output of which can be compared with the temperature measured by the sensors. The comparisons are directed into an optimization procedure identifying the coefficients. The conducted experiments take the form of fourteen 24h runs with a sampling rate of 1Hz. This generates 13Mbytes of data for each run. Histories for drain (which where actually applied to the system) are taken from the normative sheets emitted by the European norm organism (CEN [2010]) for a tank of this capacity, associated with a classical night-time heating policy until total load. Subsequent experiments consider similar total consumption but with different drain/heat combination to test the model under various situations.

The comparison of the model against data is overall satisfactory even in 24h open-loop runs, but close-up inspection reveals some possibilities of improvement.

First of all, numerical results of this model and experimental data concur and show, during heating, the appearance of a temperature plateau starting from the bottom of the

tank (see Fig. 7 (a.1)). This plateau has increasing temperature and length, but leaves temperatures at greater heights untouched and only progressively covers the whole of the tank. This phenomena is seen in experimental data in the exact same way at the exception of a small temperature backward flow observed at the higher part of plateau(see Fig. 7 (a.1)). These observations support the validity of the model, but the apparently simple dynamics of the plateau suggest some simplification could be made.

Secondly, a mismatch appears during draining in the lower part of the tank. This mismatch consists of an underestimation of the injected water temperature and a shift of the location of the layer of high temperature gradient (see Fig. 7 (a.2)), called *thermocline* (Zurigat et al. [1991]) (see Fig. 3). It is believed that these effects arise from a local mixing in the bottom of the tank, such as the one coming from a strong squirt out of the water injection nozzle. The dynamics of such mixing and its effect on the thermocline location have a strong effect on the temperature profile that cannot be reproduced by the simple convection-diffusion equation in a fixed domain. Accounting for them calls for a transformation of this fixed domain into a time-dependent one and an adaptation of boundary conditions. This work is presented in the next section.

3. HYBRID MODEL FOR HEATING, DRAINING AND HEAT LOSS

3.1 Simplifying assumptions and framework

In practice, it appears that draining and heating effects on the tank are mostly taking place over distinct periods. Therefore, the time interval on which the system is considered can be split into distinct subintervals, or phases. Introducing distinct dynamics for each phase presents the double advantage of reducing the computational burden (by tailoring numerical schemes for each dynamics) and of offering considerably more flexibility compared to a single system of PDEs.

For these reasons, we now present a hybrid model, sequencing the dynamics. These dynamics can be successively applied to the temperature profile as follows.

Consider an initial time t_0, an initial temperature profile $T_0(x)$, and a time t_c at which one wants to determine the temperature profile $T(\cdot, t_c)$. On $[t_0, t_c]$, the tank is submitted to draining and heating, characterized by the draining velocity $v_d(t)$ and the injected power $u(t)$ (related to the precedently defined P_W via the relation $u(t) = \int_0^h P_W(y,t)dy$). We assume that v_d and u are *piecewise constant and left-continuous* (at each discontinuity point).

Let us define $\mathcal{T}^u = (t_0^u = t_0, ..., t_{m_u}^u = t_c)$ and $\mathcal{T}^v = (t_0^v = t_0, ..., t_{m_v}^v = t_c)$ the sequence of discontinuity points respectively of u and v_d, and $\mathcal{T} = \mathcal{T}^u \cup \mathcal{T}^v = (t_0, ..., t_m)$ the sequence of discontinuity points of u and v_d, such that $t_0 < t_1 < ... < t_m = t_c$. This sequence $\mathcal{T}$ defines a succession of m time intervals $]t_i, t_{i+1}]$ of length Δt_i. In each time interval, the tank is in one (and only one of the configurations I, II, IIIa, IIIb defined below. Over each time interval, $u(t)$ and $v(t)$ are constant (see Fig 4).

Heating \ Draining	$v_d(t) = 0$	$v_d(t) > 0$
$u(t) = 0$	I	IIIa
$u(t) > 0$	II	IIIb

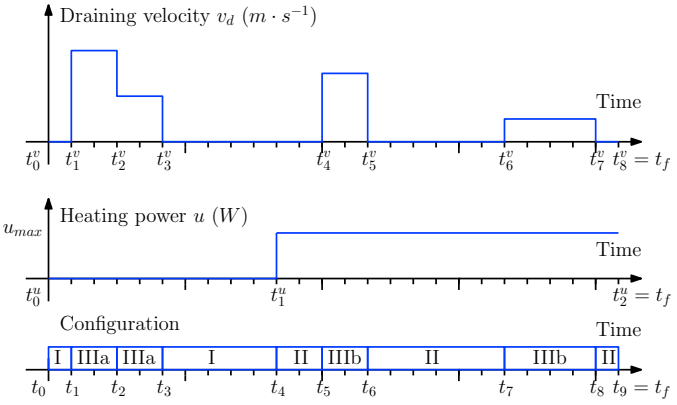

Fig. 4. Definition of the timeline

In each interval $]t_i, t_{i+1}]$, we want to determine the temperature profile as a function of time, in particular at final time t_{i+1}. This last profile will serve as initial condition for the following phase. Three functions F_I, F_{II}, F_{III} (accounting for IIIa and IIIb) map an initial profile and working conditions to temperature profiles for future times. We note,

- $T(\cdot, t_{i+1}) = F_I(T(\cdot, t_i), \Delta t_i)$
- $T(\cdot, t_{i+1}) = F_{II}(T(\cdot, t_i), \Delta t_i, u)$
- $T(\cdot, t_{i+1}) = F_{III}(T(\cdot, t_i), \Delta t_i, v_d, u)$.

Clearly, if one wishes to compute the temperature profile at any time of interest t_c, one only needs to compute the sequence of intermediate profiles $T(\cdot, t_i), i = 1, ..., m-1$ as a function of the previous ones by a chain rule. Note that for the computation on a short interval $[t_0, t_c]$ (e.g. if we focus on a succession of nearby times of interest), $\mathcal{T}$ can be reduced to a short list of events. Interestingly, a comparable split is developed in Kreuzinger et al. [2008] for the case of a water storage tank with external heating.

We now expose these mappings, for any index i.

3.2 Phase I: Rest

In this part, we consider periods without any draining or heating.

Physical considerations The only phenomena driving the temperature profile are diffusion and heat loss.

Dynamics The input variables of F_I are the initial profile, say $T_0(\cdot)$, and the duration Δt_i. They serve in the following diffusion-heat loss one-dimensional system:

$$\begin{aligned} \partial_t T &= \alpha \partial_{xx} T - k(T - T_a) && \text{on } \Omega \times I \\ \partial_x T(0,t) &= 0 && \text{on } I \\ \partial_x T(h,t) &= 0 && \text{on } I \\ T(x,0) &= T_0(x) && \text{on } \Omega \end{aligned} \tag{3.1}$$

where $I =]0, \Delta t]$ and $\Omega = [0, h]$.

We have $F_I(T(\cdot, t_i), \Delta t_i) = T(\cdot, t_{i+1})$.

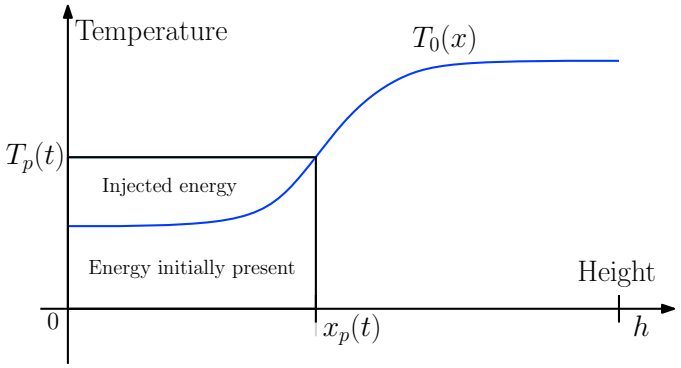

Fig. 5. Energy balance for the integral form heating model

Numerical considerations Numerically, this system can be solved relatively easily with finite difference schemes. We use a Crank-Nicholson scheme (Allaire [2007]) on a linearly spaced mesh.

3.3 Phase II: Heating

Physical considerations Heating modeling can be simplified using the appearance of the plateau discussed earlier. Turbulence generated by buoyancy effects during the heating process is the cause of a local mixing. Here, we consider that this mixing is perfect on an area $[0, x_p(t)]$, the *plateau*, and that the buoyancy effects do not affect stratification in heights above $x_p(t)$. For sake of simplicity the case without heat loss is exposed, but loss can be included without too much difficulty (this is done for the simulation presented in Section 4). To simplify the dynamics, the diffusion phenomena have to be neglected. Then, the governing equations take the form of an ODE that we derive below.

Dynamics The input variables of F_{II} are the initial profile, say $T_0(\cdot)$, the duration Δt_i, and the constant value u of the heating power. The plateau temperature is noted $T_p(t)$. It is related to $x_p(t)$ by the equation

$$T_p(t) = T_0(x_p(t)) \tag{3.2}$$

corresponding to the continuity assumption at the junction between the plateau and the (untouched) initial profile (see Fig. 5).

Denoting S the cross-section of the tank, and ρ and c_p respectively the density and heat capacity of water, an energy balance (illustrated in Fig. 5) gives

$$T_p(t)x_p(t) = \int_0^{x_p(t)} T_0(x)dx + \int_0^t \frac{u(s)}{S\rho c_p}ds \tag{3.3}$$

Denoting T_0' the derivative of T_0, relations (3.2) and (3.3) yield the dynamics of $x_p(t)$

$$\dot{x}_p = \frac{u}{S\rho c_p x_p T_0'(x_p)}, \quad x_p(0) = 0, \quad t \in]0, \Delta t] \tag{3.4}$$

which directly gives $T_p(t)$ using (3.2).

For completeness, other phenomena can be included:

- Heat loss at walls (with loss coefficient k) is a local phenomena that does not alter the shape of a plateau. Its effects are some shrinking of $T_0(\cdot)$ towards ambient temperature T_a in the form of a exponential factor e^{-kt} of the initial profile and a direct change of the dynamics of $x_p(t)$.
- If the plateau is not exactly constant but always features the same dependency in x (for instance a constant shape around the heating elements), we can divide the temperature of the plateau in two components $T_p(x,t) = T_{pt}(t) + T_{px}(x)$ and then study the dynamics of $T_{pt}(t)$.
- Finally, the small backward energy flow that is always observed (see Fig. 7 (a.1)) at the junction (in a stronger way at the top of the tank) can be modeled by breaking the continuity hypothesis (3.2) and replacing it with

$$T_p(x_p(t), t) + T_{p\Delta}(x_p(t)) = T_0(x_p(t)) \tag{3.5}$$

where the continuity gap $T_{p\Delta}$ depends of the geometry of the tank and has to be identified.

Integration of such optimal features define the dynamics of $x_p(t)$ under the general form (slightly) more complex than (3.4)

$$\dot{x}_p = f(x_p, t)u + g(x_p, t) \tag{3.6}$$

where the nonlinear functions f and g are constructed from the functions $T_0, T_{px}, T_{p\Delta}$ and their derivative or reciprocal function, and parameters S, ρ, c_p, T_a and k. Simple examples for f and g are reported in (3.4).

At any instant $t \in]0, \Delta t]$, the temperature inside the tank is defined as the profile constituted by the plateau (on the lower part) and the initial profile updated by the heat loss factor (on the upper part).

This defines $F_{II}(T(\cdot, t_i), \Delta t_i, u) = T(\cdot, t_{i+1})$.

Numerical considerations In principle, the extra features added in the dynamics could make the dynamics (3.6) difficult to identify and even more difficult to integrate. However, an integral form similar to the energy balance (3.3) gives an easy way to determine the profile at the end of the heating phase. This method is used in practice to numerically compute the profile in Section 4.

3.4 Phase IIIa and IIIb: Drain as a Stefan problem

Physical considerations During draining periods, Zurigat's convection-diffusion model (and therefore the model present in Section 2) seems to be globally valid when confronted against data, but systematic errors appear. Examination of recordings reveals that the injected water seems to be of higher temperature than the one coming from the water system, and the injection seems to be located not at $x = 0$ but at higher heights (see Fig. 7 (a.2)).

As we have seen it in Section 2, the water nozzle mixes the injected water in a volume, raising its temperature in a zone of varying size. Zurigat's model does not account for this effect and tends to neglect the water in the bottom of the tank which results in a shift of the thermocline (see Fig. 7 (a.2)). A similar effect is studied for large storage tanks ($>30\text{m}^3$) when injecting hot water on top of the tank in Oppel et al. [1986] and Nakahara et al. [1988], who introduce buffer zones of respectively constant and constantly increasing (with time) length. The buffer models they present do not yield conclusive results for our case, even though interesting similarities in the spirit of derivation can be seen with our work.

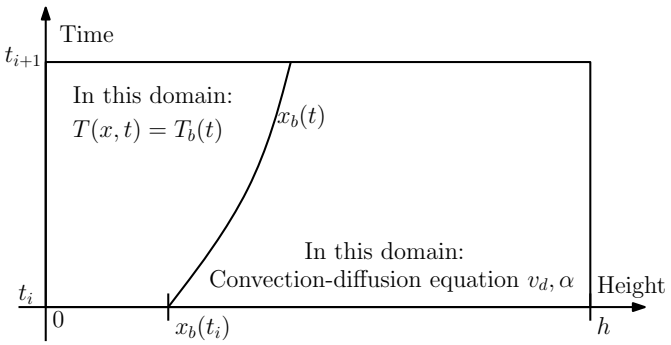

Fig. 6. The Stefan problem for modeling draining (moving boundary).

For these reasons, we introduce another homogeneous zone characterized with temperature $T_b(t)$ and length $x_b(t)$. Their dynamics are driven by the water injection. In case of simultaneous heating and draining (case IIIb), draining effects are predominant. We simply assume that the heating elements all belong to this zone and concentrate the effects of the heating power u on $T_b(t)$.

Dynamics Zurigat's convection-diffusion PDE is still valid on the interval $[x_b(t), h]$, but the Dirichlet boundary condition $T(x_b(t), t) = T_b(t)$ is now located at the end of the mixing area (x_b in Fig. 6), and thus constitutes a time-varying boundary condition.

The input variables of F_{III} are the initial profile, say $T_0(\cdot)$, the duration Δt_i, and the constant values of the heating power u and draining velocity v_d. Consider the Stefan problem

$$\begin{aligned} \partial_t T + v_d \partial_x T &= \alpha \partial_{xx} T - k(T - T_a) && \text{on } C_s \\ T(x_b(t), t) &= T_b(t) && \text{on } I \\ \partial_x T(h, t) &= 0 && \text{on } I \\ T_b(0) = T_b^0,\ x_b(0) &= x_b^0 \\ T(x, 0) &= T_0(x) && \text{on }]x_b(0), h] \end{aligned} \tag{3.7}$$

over the domain $C_s = \{(x,t) | t \in I, x_b(t) \leq x \leq h\}$ (where $I =]0, \Delta t]$).

The dynamics of T_b derive from an energy balance, i.e.

$$\begin{aligned} x_b(t)\dot{T_b}(t) = v_d[T_{in} - T_b(t)] + \alpha \partial_x T(x_b(t), t) \\ - k x_b(t)(T_b(t) - T_a) + \frac{u}{S\rho c_p}. \end{aligned} \tag{3.8}$$

For completeness, the dynamics of $x_b(t)$ are needed. There is no obvious natural way to define it (for instance from a physical principle), but observation of data suggests that the mixing zone seems to be larger when its temperature is low. Then, we choose the following general formulation

$$x_b(t) = q(T_b(t)) \tag{3.9}$$

where q is a positive, decreasing and invertible function to be identified. For the simulation, we use the nonlinear form

$$q(T) = \frac{A}{T - T_{min}} \tag{3.10}$$

where A and $T_{min} < T_{in}$ are subject to an identification procedure. More generally, q represents the mixing effects of water injection and therefore is strongly connected with the typology of the nozzle. This definition is consistent with the fact that large values of v_d will induce rapid decrease of T_b and increase of x_b.

The initial conditions x_b^0 and T_b^0 are defined as follows. The homogeneous domain is initialized with

$$x_b^0 = \text{argmin}\{x_b | \int_0^{x_b} T_0(x)dx = q^{-1}(x_b)\} \tag{3.11}$$

or $x_b^0 = h$ if the later is not defined, and $T_b^0 = q^{-1}(x_b^0)$. Then, the solution of (3.8) with (3.9),(3.11) and the coupled Stefan problem follows.

Remark 1. Generally, existence and uniqueness of such time-varying boundary conditions problem is not straightforward. Here, relating to the so-called Stefan one-phase problem (Fasano and Primicerio [1977a,b]) (which models the temperature of water next to a melting layer of ice and other crystal growth problems) and with some assumptions on q and u, we can prove not only that the problem is well-defined but also that for any time $t \in I$, $T(\cdot, t)$ is an increasing function. The proof of this result is out of scope of this paper, but will be the subject of future publications.

Remark 2. If $\exists t \in [0, \Delta t]$ s.t. $x_b(t) = h$, the previously defined dynamics is stopped and is replaced for later times by

$$\begin{aligned} h\dot{T_b}(t) &= v_d[T_i - T_b(t)] - kh(T_b(t) - T_a) + \frac{u}{S\rho c_p} \\ x_b(t) &= h \end{aligned} \tag{3.12}$$

defining $T(\cdot) = T_b(t)$ over the whole domain.

The description above defines the function F_{III}: given a constant draining v_d and heating u, F_{III} is the mapping from $T_0(\cdot), \Delta t_i, v_d$ and u to the solution $T(\cdot, s)$ of (3.7),(3.8),(3.9) at time t_{i+1}. In other words

$$F_{III}(T(\cdot, t_i), \Delta t_i, u, v_d) = T(\cdot, t_{i+1}).$$

Numerical considerations As in section 3.2, this system can be solved numerically with finite difference schemes, jointly with an ODE solver for the state T_b. However, attention has to be paid to the moving boundary to ensure consistency of the numerical scheme.

3.5 Summary of the model

The definitions of functions F_I, F_{II}, F_{III} above allow an easy computation of the temperature profile at any final time t_c: given a succession of phases separated by times $\mathcal{T} = (t_0, t_1, ..., t_m = t_c)$ and an initial profile $T(\cdot, t_0)$, intermediary profiles $T(\cdot, t_i)$ are computed by successive applications of the functions, using the constant values of u and v_d during each phase.

Remark 3. If we define $E \subset L^\infty(\Omega)$ the set of increasing, piecewise continuous and continuously piecewise differentiable functions, with some assumptions on u, then each of F_I, F_{II}, F_{III} maps the profiles from E to E, ensuring that our problem is well-defined.

4. MODEL VALIDATION

The second model has been compared against experimental data in the same conditions as the first. An additional set of data has been generated for a total of twenty runs,

reduced to eight after elimination of corrupted and redundant data. Comparison with numerical results shows clear improvements both during draining parts (with the vanishing of the temperature and thermocline shifts) (see. Fig 7 (a.2)(b.2)) and during heating parts (with a better estimation of the plateau distribution and the backward flow) (see. Fig 7 (a.1)(b.1)). The changes have a positive impact on the accuracy of the model, as is reported in Table 2, in which the statistics of the absolute difference between simulation and experimental data has been used as a quality index (for the whole set of data): with the hybrid model, 96.8% of predicted temperature have an error lower than 4^oC.

Table 2. Comparison of absolute difference between experimental value and model prediction; computational time. Percentage of sample for each error interval. M1: First model, M2: Hybrid model

Err.	0-2^{o}C	2-4^{o}C	4-6^{o}C	6-8^{o}C	8^{o}C+	Time
M1	53.9%	22.9%	10.7%	5.1%	7.4%	2435.6s
M2	82.3%	14.5%	2.0%	0.6%	0.6%	4.6s

5. CONCLUSION

This paper proposes a new model for an EHWT. This model is based on experimental observations. It has the advantages of being accurate and computationally light. This model opens doors to optimization of heating policies, by enabling accurate and fast computation of any comfort indicator defined from the internal temperature profile, which can be used as objective function. In Fig. 8, we report the prediction of the introduced "available energy", contained in the EHWT. Experimental data are well reproduced (over 24h) by our model. A simplistic integration model is shown, for comparisons, which clearly demonstrate the relevance of our approach.

REFERENCES

Aguilar, C., White, D., and Ryan, D.L. (2005). Domestic water heat and water heater energy consumption in Canada. Technical report, Canadian BEEU Data and Analysis Centre.

Allaire, G. (2007). *Numerical Analysis and Optimization*. Oxford University Press.

Beeker, N., Malisani, P., and Petit, N. (2015). A distributed parameters model for electric hot water tanks. In *Proceedings of the American Control Conference*.

Blandin, D. (2010). *Modélisation et validation expérimentale de nouveaux concepts de ballons solaires à forte stratification*. Ph.D. thesis, Insa Lyon.

CEN, T.C. (2010). Heat pumps with electrically driven compressors - Testing and requirements for marking for domestic hot water units. Technical report, European Committee for Standardization.

Commission, E. (2011). Energy roadmap 2050: communication from the commision to the European parliament, the council, the European economic and social committee and the committee of the regions. Technical report, UE.

Dincer, I. and Rosen, M.A. (2010). *Thermal Energy Storage: Systems and Applications*. John Wiley & Sons.

Edenhofer, O., Pichs-Madruga, R., Sokona, Y., and Seyboth, K. (2011). IPCC special report on renewable energy sources and climate change mitigation. Technical report, Intergovernmental Panel on Climate Change.

Fasano, A. and Primicerio, M. (1977a). General free-boundary problems for the heat equation. *Journal of Mathematical Analysis and Applications*.

Fasano, A. and Primicerio, M. (1977b). General free-boundary problems for the heat equation, ii. *Journal of Mathematical Analysis and Applications*.

Han, Y., Wang, R., and Dai, Y. (2009). Thermal stratification within the water tank. *Renewable and Sustainable Energy Reviews*, 13, 1014–1026.

Johannes, K., Fraisse, G., Achard, G., and Rusaouën, G. (2005). Comparison of solar water tank storage modelling solutions. *Solar Energy*, 79, 216–218.

Klein, S., Beckman, W., and Mitchell, J. (2010). TRNSYS - Reference manual. Technical report, Solar Energy Laboratory, University of Wisconsin-Madison.

Kleinbach, E., Beckman, W., and Klein, S. (1993). Performance study of one-dimensional models for stratified thermal storage tanks. *Solar Energy*, 50, 155–166.

Kreuzinger, T., Bitzer, M., and Marquardt, W. (2008). Mathematical modelling of a domestic heating system with stratified storage tank. *Mathematical and Computer Modelling of Dynamical Systems*, 14(3), 231–248.

Lavan, Z. and Thompson, J. (1977). Experimental study of ththermal stratified hot water storage tanks. *Solar Energy*.

MSI (2013). Marché des équipements domestiques de production d'ECS en France. Technical report, MSI Reports.

Nakahara, N., Sagara, K., and Tsujimoto, M. (1988). Initial formation of a thermocline in stratified storage tanks. *ASHRAE Transactions*, 371–394.

Oppel, F., Ghajar, A., and Moretti, P. (1986). Computer simulation of stratified heat storage. *Applied Energy*, 23, 205–224.

Palensky, P. and Dietrich, D. (2011). Demand side management: Demand response, intelligent energy systems, and smart loads. *IIIE Transactions on Industrial Informatics*.

Ryan, D., Long, R., Lauf, D., and Ledbetter, M. (2010). Water heater market profile. Technical report, U.S. Department of energy.

Zurigat, Y., Ghajar, A., and Moretti, P. (1988). Stratified thermal storage tank inlet mixing characterization. *Applied Energy*, 30, 99–111.

Zurigat, Y., Liche, P., and Ghajar, A. (1991). Influence of inlet geometry on mixing in thermocline thermal energy storage. *Int. J. Heat Mass Transfer*, 34, 115–125.

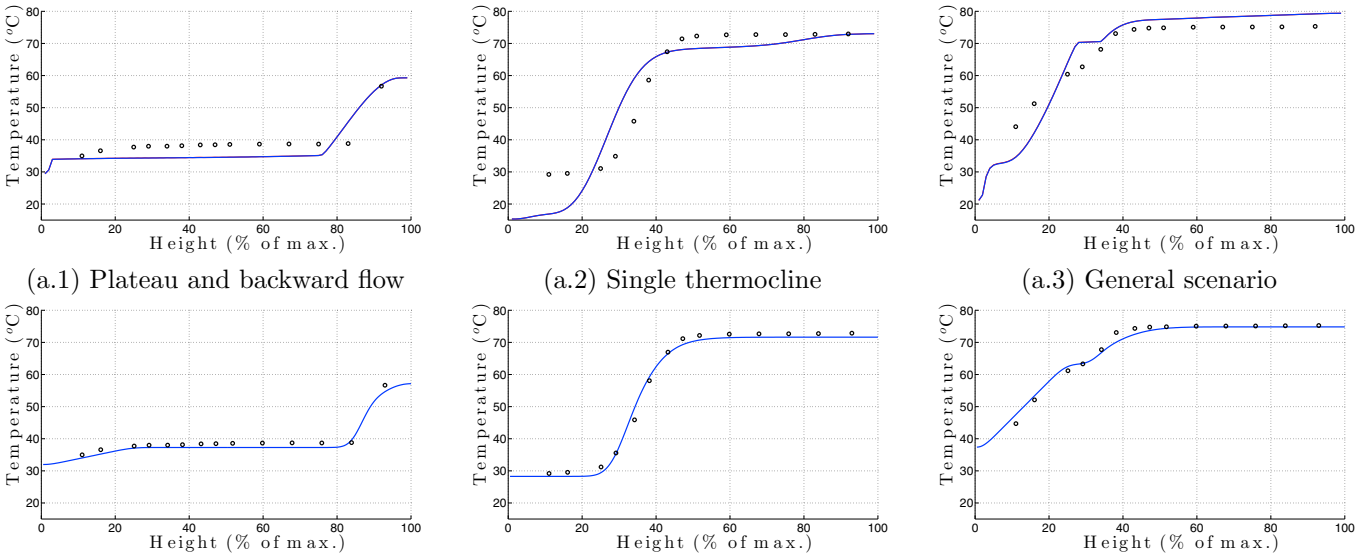

(a.1) Plateau and backward flow (a.2) Single thermocline (a.3) General scenario

(b.1) Plateau and backward flow (b.2) Single thermocline (b.3) General scenario

Fig. 7. Comparisons of the first model (a) and the hybrid model (b), against experimental data (black), simulation are in blue.

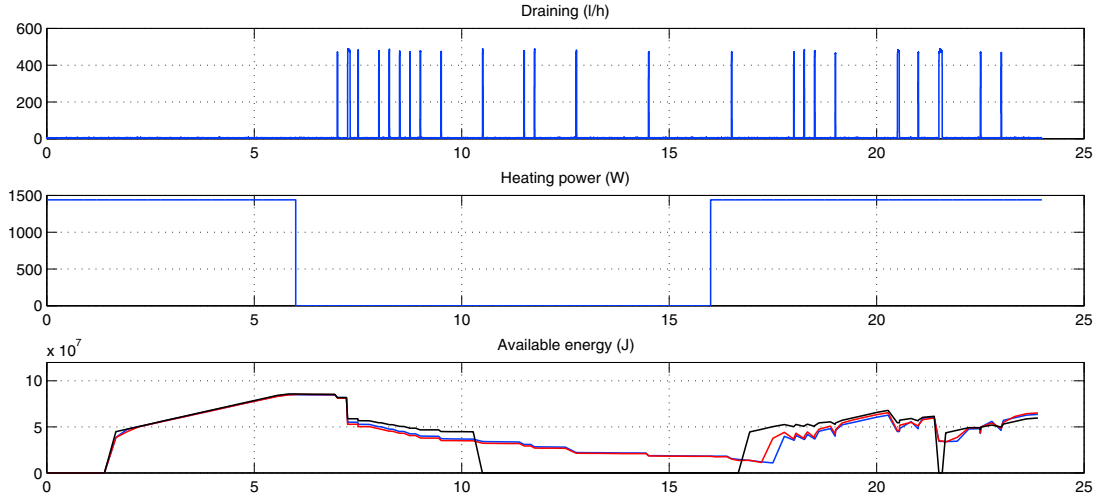

Fig. 8. Simulation of the "available energy" contained in the EHWT. Using the histories of draining and heating, and a uniform cold profile as initial condition, the proposed model kindly reproduces experimental data while vastly outperforming a simplistic single-integrator model. Red: experimental data, blue: model predictions, black: single-zone model.